Preparation and characterization of Ca(II) cross-linking modified pectin microspheres for Pb(II) adsorption

Fen Li, Zhao Xu, Xiaoyan Wen, Xiaoyong Li, Yanhong Bai and Jianjun Li

ABSTRACT

A novel adsorbent, composed of cross-linked de-esterified pectin microspheres, was prepared via cross-linking with Ca(II) and modification by de-esterified pectin, low-methoxyl pectin (LMP) and pectic acid (PA). Fourier transform infrared (FTIR), energy dispersive spectrometry (EDS), scanning electron microscopy (SEM) and atomic absorption spectroscopy (AAS) were applied too, exhibiting a successful fabrication, good adsorption ability, and well-defined surface microstructure beneficial to Pb(II) adsorption. The adsorption ability of pectin microspheres (PMs), low-methoxyl pectin microspheres (LMPMs) and pectic acid microspheres (PAMs) for Pb(II) in aqueous solution were explored. The maximum adsorption capacity of PMs, LMPMs and PAMs was 127 $mg \cdot g^{-1}$, 292 $mg \cdot g^{-1}$ and 325 $mg \cdot g^{-1}$ at pH 5.0 respectively, indicating a great improvement of LMPMs and PAMs in the adsorption ability for Pb(II) compared with PMs. Furthermore, the adsorption mechanism was proposed. The experimental data were well fitted with pseudo-second-order kinetic and Langmuir isotherm models. Five-cycle reusability tests demonstrated that microspheres could be used repeatedly. All the results confirmed that LMPMs and PAMs, which presented outstanding adsorption capability and reusability, could be a good candidate for wastewater purification.

Key words | adsorption, mechanism, microsphere, Pb(II) ion, pectin

Fen Li
Zhao Xu
Xiaoyong Li
Yanhong Bai
Jianjun Li (corresponding author)
Department of Chemistry, School of Science,
Xi'an Jiaotong University,
Xi'an 710049,
China
E-mail: *li.jianjun@xjtu.edu.cn*

Xiaoyan Wen
Xi'an Modern Chemistry Research Institute,
Xi'an 710065,
China

INTRODUCTION

Pb(II), Hg(II) or Cd(II) and other heavy metal pollution have attracted worldwide attention, due to its special properties in terms of strong diffusibility, high toxicity and nonbiodegradability (Jorgetto *et al.* 2015). Generally, heavy metals, which transferred to the human body through food chains from water body, would cause various physical diseases or disorders (Chojnacka 2010). The research had already demonstrated that Pb(II) accumulates in the brain and nervous system leading to deformity, besides limb numbness and movement disorder are caused by Hg(II) and Cd(II) (Blumenthal *et al.* 1995; Rice *et al.* 2014). Therefore, researchers engaged in environmental safety have been seeking more reasonable materials for water pollution.

The ways for removal of heavy metals mainly include chemical precipitation (España *et al.* 2006), adsorption (Shariful *et al.* 2017), membrane filtration (Mortaheb *et al.* 2010), ion-exchange (Fonseca *et al.* 2005), electrodialysis (Mohammadi *et al.* 2005), and flocculation (Dineshkumar *et al.* 2008). Due to its efficiency, economy, reproducibility, and environmental friendliness, adsorption is a preferred method in these techniques (Yang *et al.* 2014). Chemisorption is the main adsorption mode because some adsorbents' functional groups can chelate with metal ions, usually including some coordination atoms (Liao *et al.* 2016). However, in the treatment of water contaminated with trace heavy metal ions, these techniques tend to be expensive or inefficient. Nowadays, biosorption is thought to be a more appropriate method compared with traditional methods because it has the characteristics of good economic, social and ecological benefits. The adsorbents, such as pectin, chitosan or sodium alginates, are crucial (Li & Buschle-Diller 2017) not just because of its excellent adsorption and economic performance, but there is no secondary pollution (Chen & Wang 2008; Wang & Chen 2014). According to reports (Khotimchenko *et al.* 2008; Celus *et al.* 2017), pectin is regarded as a suitable candidate among available adsorbents. In this study, pectin and the modified pectin were used to remove the heavy metal in aqueous solution.

Pectin substances are the ionic plant polysaccharides, whose main structural features are linear chains containing

doi: 10.2166/wst.2019.151

more than 100 (l-4)-linked α-D-galacturonic acid residues (Liu *et al.* 2003). Pectin has called attention mainly due to its unique properties, such as biodegradability, biocompatibility, nontoxicity, and adsorption property, proved in numerous studies (Serguschenko *et al.* 2007). Since pectin is mostly extracted from the residues of sugar beet, citrus and apple which is abundant and cheap, waste utilization can be realized. Pectin, however, had a low adsorption capacity when directly used to remove heavy metal ions. It was one possible way to improve the adsorption ability by modifying the structure of pectin substances (Assifaoui *et al.* 2015).

In this study, the work aims at investigating the adsorption ability of the modified pectin, including LMP and PA which were prepared from pectin by pH-modification. The microspheres were characterized by a series of structural characterization (scanning electron microscopy (SEM), energy dispersive spectrometry (EDS) and Fourier transform infrared (FTIR)). Batches of experiments were performed to estimate its adsorption capacities for Pb(II) in aqueous solutions at various pH values, contact time, and initial concentrations. Furthermore, three kinds of adsorption kinetics and two kinds of adsorption isotherms were used to further explore the uptake behavior of different microspheres. Its adsorption-desorption performance was also investigated. The results show that the adsorption abilities of LMPMs and PAMs are higher than that of PMs and their high adsorption performance would provide great potential for wastewater treatment.

MATERIAL AND METHOD

Materials

Citrus pectin (CAS: 9000-69-5, galacturonic acid ≥74.0%) was purchased from Sigma Biotechnology Co. (USA). $Pb(NO_3)_2$, $CaCl_2$ and $CdCl_2{\cdot}2.5H_2O$ were from Xi'an Chemical Reagent Factory (Shaanxi, China). All reagents were of analytical grade, and the deionized water with a resistivity of 18 M cm (Milli-Q Biocel A10, Millipore, USA) was used throughout.

Preparation of LMP and PA

The preparation of LMP was performed as Fraeye described (Ilse *et al.* 2009). The PA was prepared by the similar method mentioned above. Briefly, 10 g citrus pectin power was dissolved in 500 mL 1.0 mol L^{-1} NaOH ethanol solution (95%, v/v) via a magnetic stirring at 4 °C for 5 h. The solution was passed through a membrane filter overnight and the residue was dissolved in 50% ethanol (v/v), followed by adding 3 mol L^{-1} HCl to adjust the pH 1.5. After placing it at room temperature for 1.5 h, the solution was filtered and the residue was dissolved in 250 mL 50% ethanol (v/v, containing 1% HCl) with constant stirring at 25 °C for 0.5 h. The PA was obtained, then the mixture was filtered and the precipitate was washed with 50% ethanol (v/v) three times.

Preparation PMs, LMPMs and PAMs

Pectin solution was prepared by dissolving 0.3 g of pectin power in 10 mL of deionized water (3%, w/v). Using syringe (1 mL, 0.45 #) added the pectin solution to the calcium chloride solution (10%, w/v) dropwise, the needle was about 5 cm from the liquid level. After 20 min, PMs were collected through a membrane filter separation, and then washed thoroughly by deionized water. LMPMs and PAMs were prepared using the same procedure as PMs, except the concentration of calcium chloride solution was used as 5%.

Characterization of PMs, LMPMs and PAMs

FTIR spectra of PMs, LMPMs and PAMs were obtained by an FTIR spectrometer (Nicolet AVATAR 360, Thermo Instrument Company, Madison, WI, USA) at the wave number range of 400–4,000 cm^{-1}. SEM (TM-1000 SEM, Hitachi, Japan) was used to observe the surface microstructure and morphology of PMs, LMPMs, PAMs or microspheres-Pb(II). Elemental mapping images of three kinds of microspheres before and after Pb(II) adsorption were obtained using a scanning electron microscopy-energy dispersive spectrometer (SEM-EDS, Quantax70, Bruker, Germany).

Adsorption experiments

All the adsorption experiments in single or binary system were conducted in an Erlenmeyer flask on a magnetic stirrer at 25 °C to determine the adsorption capabilities, kinetic and thermodynamic parameters of microspheres. After adsorption, the solution was filtered through 0.22 μm syringe filter. The remaining content of metal ions was measured by a flame atomic absorption spectrophotometer (AA1700, FULI Instrument, China). The adsorption capacity (q_e) was calculated by Equation (1).

$$q_e = \frac{(C_0 - C_e)V}{m} \tag{1}$$

where q_e (mg·g^{-1}) is the adsorption capacity, C_0 (mg·L^{-1}) and C_e (mg·L^{-1}) are initial and final concentrations of

metal ions, respectively. V (L) is the volume of the metal ion solution, and m (g) is the mass of the dried adsorbent.

The experiments on effect of pH were performed at initial pH 1.0–6.0 of Pb(II) solution with initial concentration of 130 mg·L^{-1} for 240 min. The experiments on influence of contact time were conducted for 10, 20, 30, 60, 90, 120, 150, 180, 210, and 240 min with initial Pb(II) concentration of 130 mg·L^{-1} at pH 5.0. The experiments on impact of initial Pb(II) concentration were carried out with concentrations of 50, 100, 150, 200, 250, 300, 350, 400, 450, 500, 600, 700 mg·L^{-1} at pH 5.0 for 150 min.

Selective adsorption

The tests of selective adsorption were carried out in a binary ion mixture system of Cd(II) and Pb(II). A total of 50 mg of microspheres was added into 100 mL of the mixed solution with 250 mg·L^{-1} of initial concentration of Cd(II) and Pb(II) at initial pH 5.0, after continuous stirring for 150 min, the residual concentration of Cd(II) or Pb(II) was measured. Each test was conducted in triplicate.

Desorption and regeneration

After adsorption for Cd(II) and Pb(II), the microspheres were collected and washed thoroughly with deionized water at least five times to remove unabsorbed metal ions on the surface. The metal-loaded microspheres were constantly stirred in 0.002 mol L^{-1} Na_2EDTA solution to desorption for 1 h. Then, the microspheres were filtered and washed thoroughly until Cd(II) and Pb(II) concentration in the filtrate was close to zero. The collected microspheres were further used in the next adsorption cycle. The regeneration tests were conducted for five times under the same conditions to evaluate the reusability of microspheres.

Statistical analysis

The experiments were carried out in triplicate, and the results are presented as the means ± SD (standard deviation) ($n = 3$).

RESULTS AND DISCUSSION

Characteristic of pectin substance and microspheres

DE and FTIR analysis

The degree of esterification (DE) is a key parameter for pectin substance when they are considered to have the behaviors as the ion-exchange properties, water-binding capacity, cross-linking with calcium ions and the assembly of hydrogen bonding. The main structural characteristics of all pectin substances is DE, indicating the number of galacturonic acid residues with methanol radicals attached. In this work, DE of three citrus pectin samples, pectin, LMP and PA, was determined using titrimetric method (Afanas'Ev *et al.* 1984) to evaluate the modification of pectin substance and the results are shown in Table 1.

Table 1 | The DE of three citrus pectin samples

Sample	Pectin	LMP	PA
DE(%)[a]	47.90 ± 0.60	18.04 ± 0.70	0.90 ± 0.30

[a]Data shown are the means ± SD, $n = 3$.

To preliminarily investigate the chemical structure of the modified pectin and synthesis process of microspheres, FTIR analysis was carried out, and the results are shown in Figure 1. The main characteristic absorption bands of pectin were summarized as follows: 3,346 cm^{-1} (stretching vibration of O-H), 1,731 cm^{-1} (C = O stretching vibration of ester group), 1,607 cm^{-1} (C = O stretching vibration of carboxyl groups) (Iqbal *et al.* 2009). Compared with pectin spectrum (Panda *et al.* 2008), the spectrum of LMP was changed significantly: the bands at 1,730 cm^{-1} (C = O) became weaker and at 1,600 cm^{-1} (C = O) became stronger respectively, demonstrating that the ester groups in pectin become carboxyl groups partly; in the spectrum of PA, the bands at 1,607 cm^{-1} (C = O) shifted to 1,730 cm^{-1} demonstrating that the carbonyl in ester groups and carboxyl groups were overlaid and the ester groups was taken out. These changes above implied that DE of LMP and PA was reduced successfully, which was in accordance with the results shown in Table 1.

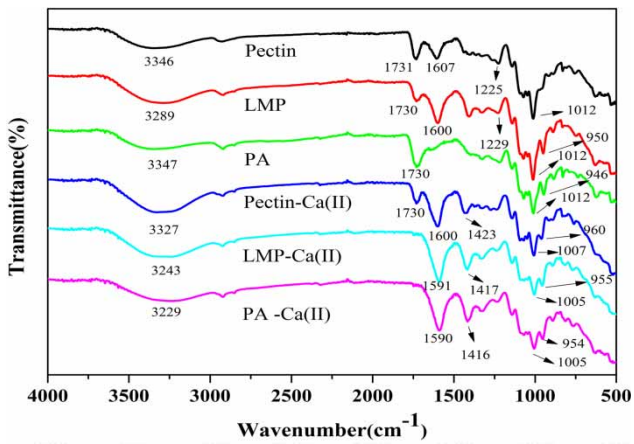

Figure 1 | FTIR spectra of pectin, LMP, and PA before and after crosslinking with Ca(II) (the arrows indicate absorption peaks).

For pectin-Ca(II), a new band at 1,423 cm^{-1} appeared and the intensity at 3,327 cm^{-1} became weaker, compared with pectin spectrum. For LMP-Ca(II), the bands at 3,243 cm^{-1} (O-H) changed and 1,591 cm^{-1} (O-H) emerged compared with LMP spectrum. For PA-Ca(II) spectrum, new bands at 1,416 cm^{-1} appeared and 3,229 cm^{-1} dropped off compared with PA spectrum, indicating that pectin, the LMP and PA had a cross-linking reaction successfully with Ca(II).

SEM observation

As shown in Figure 2, the images of PMs, LMPMs and PAMs at different magnification were recorded via SEM, by which the surface morphology and texture of each sample was mapped out. As shown in Figure 2(a), PMs' surface with uniform folds exhibited homogeneity and small cracks. The mean diameters of three microspheres all were 2 mm and had an integral surface, which could facilitate the separation and recycling of samples.

Adsorption capacity of microspheres

Adsorption of Pb(II)

Pectin products in the form of microspheres can increase specific surface area and expose more reaction sites to combine with heavy metals directly to a certain extent (Zhang *et al.* 2017b). Then, it is easy to operate in use and facilitate reusing operation, unlike nanoparticles or powders (Dragan *et al.* 2014b). Moreover, the adsorption ability of microspheres increases sharply via decreasing the DE.

Smoother surfaces of PMs without any conspicuous cracks after Pb(II) adsorption (Figure 2(b)) were observed compared with the raw microspheres (Figure 2(a)), which might be due to the accumulation of Pb(II) through adsorption. The microspheres' cracks became fewer with the decrease of the DE. Element distributions after Pb(II) adsorption showed that Pb was presented in the image and distributed homogeneously comparing to the image of raw microspheres. The Pb element in Figure 2(a) is background. This confirmed that Pb was adsorbed and that the active sites distributed uniformly on the surface of microspheres. EDS measurement exhibited (Figure 3) that the content of Ca decreased apparently, indicating a ligand-exchange between the coordinated Pb and Ca. The LMPMs and the PAMs showed performance similarly. Thus, the pectin and the modified pectin had an absorption for Pb(II), evidently. The adsorption mechanism could be regarded as the coordination effect between Pb and hydroxyl groups (–OH), and ligand exchange between Pb and Ca.

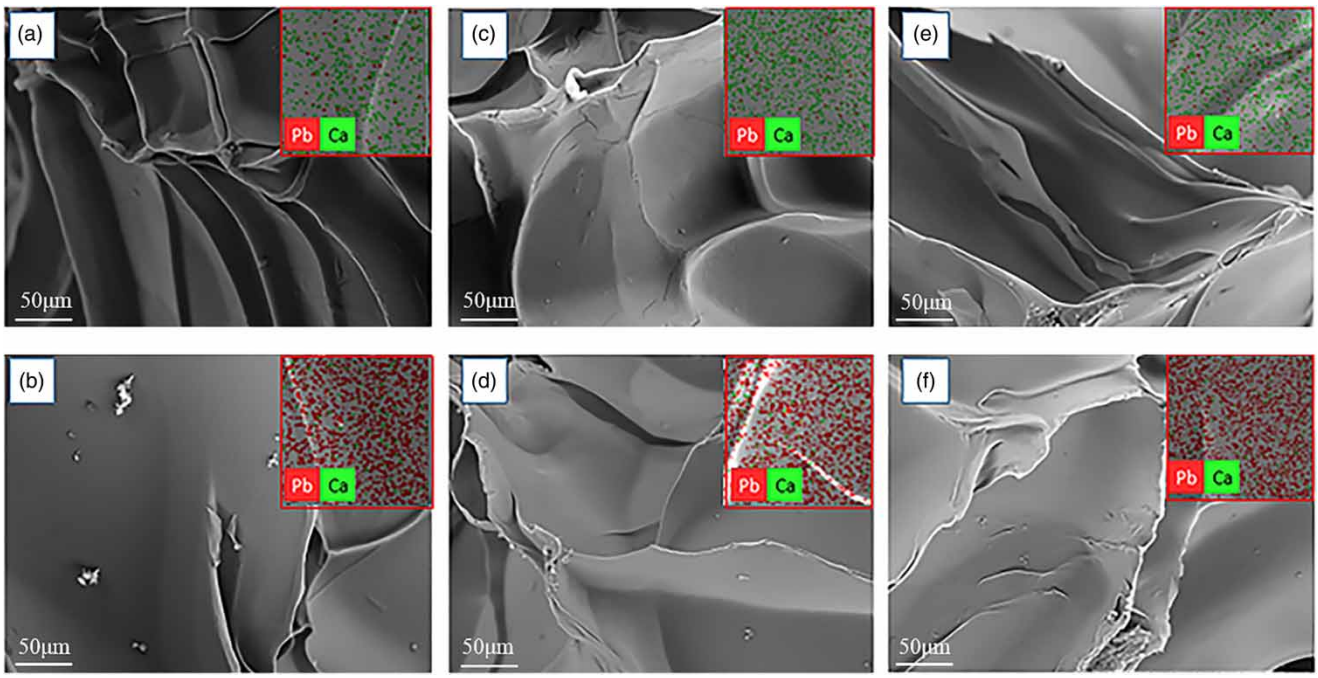

Figure 2 | SEM and element mapping (inside) images of PMs (a and b), LMPMs (c and d) and PAMs (e and f) before (a, c, e) and after the adsorption of Pb(II) (b, d, f).

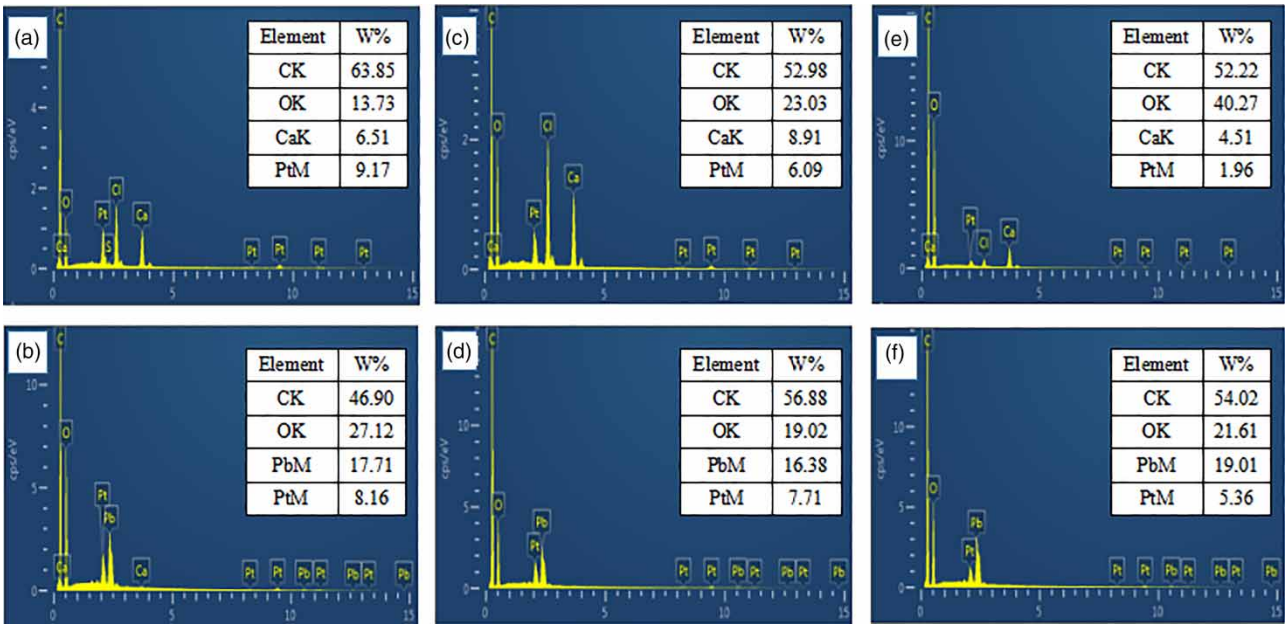

Figure 3 | EDS spectra of PMs (a and b), LMPMs (c and d) and PAMs (e and f) before (a, c, e) and after the adsorption of Pb(II) (b, d, f).

Effect of pH on adsorption

The initial pH of aqueous solutions is an important parameter that greatly influences the adsorption property of an adsorbent (Dragan *et al.* 2014a). For PMs, LMPMs and PAMs, the impacts of pH 1.0–6.0 on the adsorption for Pb(II) are displayed in Figure 4(a). Due to the protonated degree of hydroxy groups, the adsorption capacity of three absents were poor at a lower pH, because of the strong electrostatic repulsion between adsorption sites and metallic ions and competition between hydronium ions and metal ions for adsorption sites (Khormaei *et al.* 2007). At pH 6, the adsorption rate of PMs, LMPMs and PAMs for Pb(II), respectively, reached maximum values, about 69%, 92% and 95%, respectively. When the value of pH in the solution reached to 6.0, Pb(II) have tended to precipitate. There would be less Pb(II) remaining consequently, showing a high adsorption rate in the result. The initial pH of the Pb(II) solution is close to pH 5, while the adsorption rate of the microspheres at pH 4 is almost equal to that of them at pH 5, so the optimization of pH in the equilibrium adsorption is 5.

Adsorption mechanism

Effect of contact time and adsorption kinetics

Figure 4(b) exhibits the effect of contact time on Pb(II) adsorption on three kinds of microspheres. After 90 min, the amount of adsorption of PMs, LMPMs and PAMs on Pb(II) were 74%, 90% and 96%, respectively. Then, the adsorption capacities increased slowly with the increase of contact time until reaching adsorption equilibrium at 150 min. It was a slow process in which the metal ion diffusion into pores and the adsorption by interior surface while almost all facial adsorption sites of microspheres have been occupied.

To explore adsorption behavior, both pseudo-first-order and pseudo-second-order kinetic models were used to fit adsorption data, as shown in Table 2. Generally, the linear pseudo-first-order, pseudo-second-order models and intraparticle diffusion models are respectively expressed by Equations (2)–(4) below.

$$\ln(q_e - q_t) = \ln(q_e) - k_1 t \tag{2}$$

$$\frac{t}{q_t} = \frac{1}{k_2 q_e^2} + \frac{t}{q_e} \tag{3}$$

$$q_t = k_p t^{\frac{1}{2}} + C \tag{4}$$

where k_1 (min^{-1}), k_2 ($\mathrm{g{\cdot}mg^{-1}{\cdot}min^{-1}}$), and k_p ($\mathrm{mg{\cdot}g^{-1}{\cdot}min^{-1/2}}$) represent the rate constants of pseudo-first-order, pseudo-secondorder, and intraparticle diffusion models, respectively. q_e ($\mathrm{mg{\cdot}g^{-1}}$) and q_t ($\mathrm{mg{\cdot}g^{-1}}$) are the mass of Pb(II) adsorbed by per gram microspheres at equilibrium time and t (min), respectively. C ($\mathrm{mg{\cdot}g^{-1}}$) is an intraparticle diffusion constant.

The corresponding kinetic parameters of three models are listed in Table 2. Clearly, the values of correlation

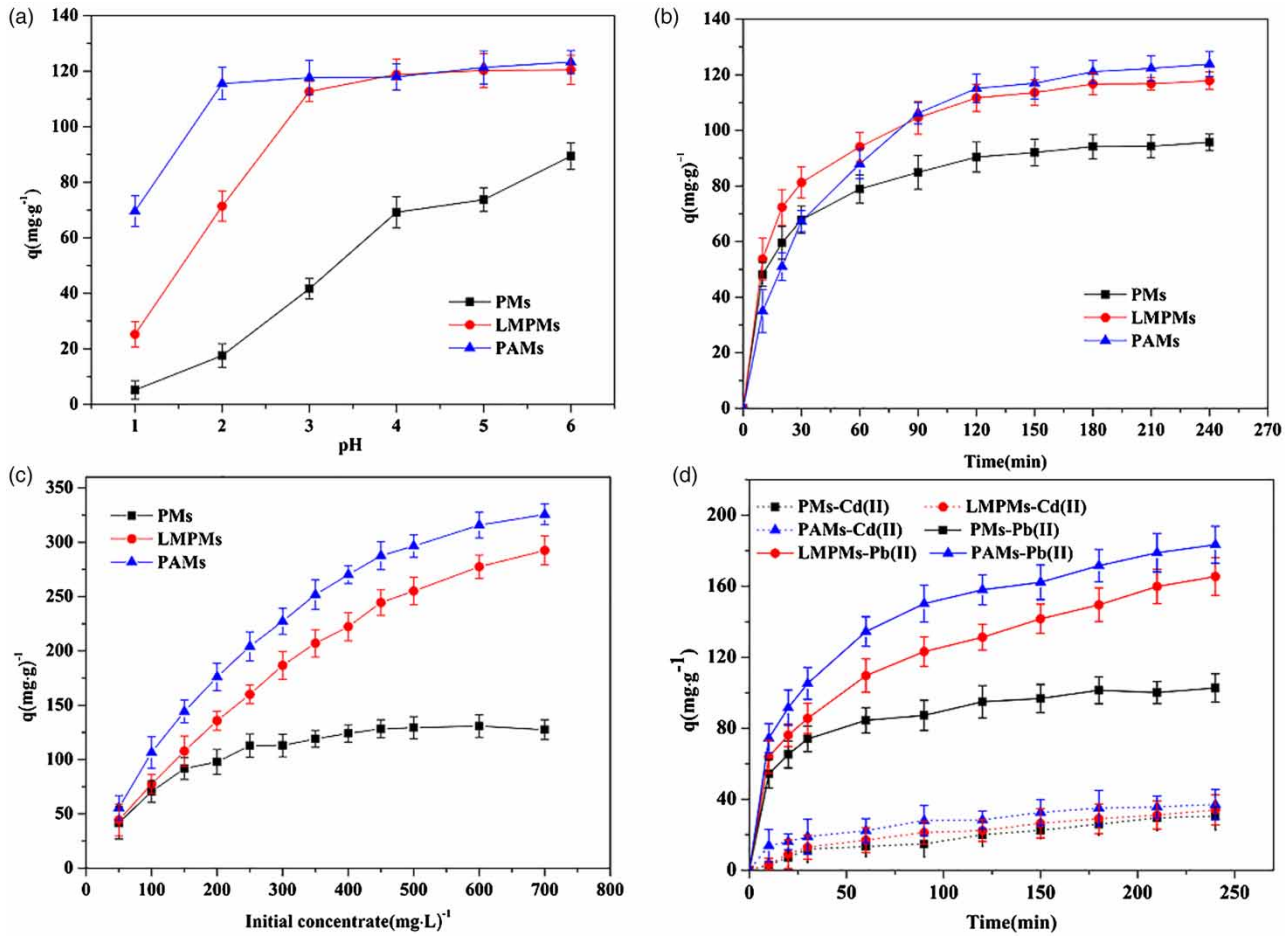

Figure 4 | Effects of initial pH (a), contact time (b), initial concentrations (c) on adsorption and selective adsorption (d) of microspheres toward Cd(II) and Pb(II).

coefficient (R^2) of three kinds of microspheres indicated the data were fitted better by pseudo-second-order model than by pseudo-first-order model, suggesting that pseudo-second-order model could well interpret the adsorption procedure, which was mainly a chemical adsorption. The intraparticle diffusion model is mainly used to verify whether the intraparticle diffusion is a rate limiting step in whole adsorption process. The values of R^2 of the intraparticle diffusion model was very low, so the model was not fit for the experimental data. These results suggested that the

Table 2 | Kinetic model and parameters of the adsorption for Pb(II) on three kinds of microspheres

Kinetic model	Parameter	PMs	LMPMs	PAMs
Pseudo-first-order model	$q_e$exp (mg·g^{-1})	95.74	117.87	123.84
	K_1 (min^{-1})	1.81×10^{-2}	2.08×10^{-2}	2.01×10^{-2}
	$q_e$cal (mg·g^{-1})	51.47	75.79	107.49
	R_1^2	0.9886	0.9817	0.9793
Pseudo-second-order model	K_2 (g·mg^{-1}·min^{-1})	6.90×10^{-4}	4.93×10^{-4}	2.10×10^{-4}
	$q_e$cal	101.01	125.79	142.04
	R_2^2	0.9995	0.9993	0.9987
Intraparticle diffusion	K_p (mg·g^{-1}·min$^{-1/2}$)	5.221	6.6424	8.064
	C (mg·g^{-1})	27.27	30.78	14.98
	R^2	0.8085	0.8339	0.9281

pseudo-second-order model was the best one to describe Pb(II) adsorption of the microspheres, so chemical adsorption was a rate limiting step in this adsorption system but not the intraparticle diffusion.

Effect of initial concentration and adsorption isotherm

The effects of the initial Pb(II) concentration on the adsorption of the microspheres are shown in Figure 4(c). For LMPMs and PAMs, the amount of the adsorbed ions increased slowly until it approached the plateau at $C_0 =$ 600 mg·L^{-1}. The maximum adsorption capacity of LMPMs and PAMs were 292 mg·g^{-1} and 325 mg·g^{-1}, respectively. Obviously, it was about 2.5 times as much as that of PMs (127 mg·g^{-1}), which indicated the ability of chelating with metal ions of LMPMs and PAMs was significantly improved by decreasing the DE within the experimental.

The equilibrium isotherm model is fundamental in describing interactive behavior between metal ions and adsorbents. The adsorption isotherms of PMs, LMPMs and PAMs for Pb(II) were determined by Langmuir and Freundlich isotherms. The Langmuir and Freundlich isotherms are respectively described by Equations (5) and (6) below.

$$\frac{C_e}{q_e} = \frac{1}{q_m k_L} + \frac{C_e}{q_m} \tag{5}$$

$$q_e = k_F C_e^{\frac{1}{n}} \tag{6}$$

where C_e (mg·L^{-1}) is the equilibrium concentration of metal ions in solution, q_e (mg·g^{-1}) is the adsorption capacity at equilibrium, q_m (mg·g^{-1}) is the maximum adsorption capacity, K_L (L·mg^{-1}) and K_F (mg$^{1-1/n}$ ·L$^{1/n}$ ·g^{-1}) are Langmuir and Freundlich constants, respectively, and n is Freundlich exponent related to adsorption intensity.

As shown in Figure 5, the fitting linear showed that the data were fitted better by Langmuir isotherm than by Freundlich isotherm, suggesting that Langmuir isotherm model could well interpret the adsorption procedure, which was mainly a monolayer adsorption on surface with the finite number of identical sites.

Undeniably, Langmuir isotherm model was the best one to illustrate the adsorption behavior between microspheres and Pb(II). In Langmuir isotherm model, the affinity between adsorbent and metal ions can be predicted by a dimensionless separation factor R_L, which is defined as Equation (7).

$$R_L = \frac{1}{1 + K_L C_0} \tag{7}$$

where C_0 (mg·L^{-1}) is the initial concentration of the metal ions, K_L(L·mg^{-1}) is Langmuir constant, R_L demonstrates the adsorption nature, which can be divided as irreversible ($R_L = 0$), favorable ($0 < R_L < 1$), linear ($R_L = 1$), and unfavorable ($R_L > 1$).

In the experiment, $K_L > 0$, thus, all the values of R_L were in the range of 0–1, indicating that the adsorption process for Pb(II) was favorable in the single metal ion system. Therefore, the microspheres used in the work were the favorable adsorbent under the experimental concentrations.

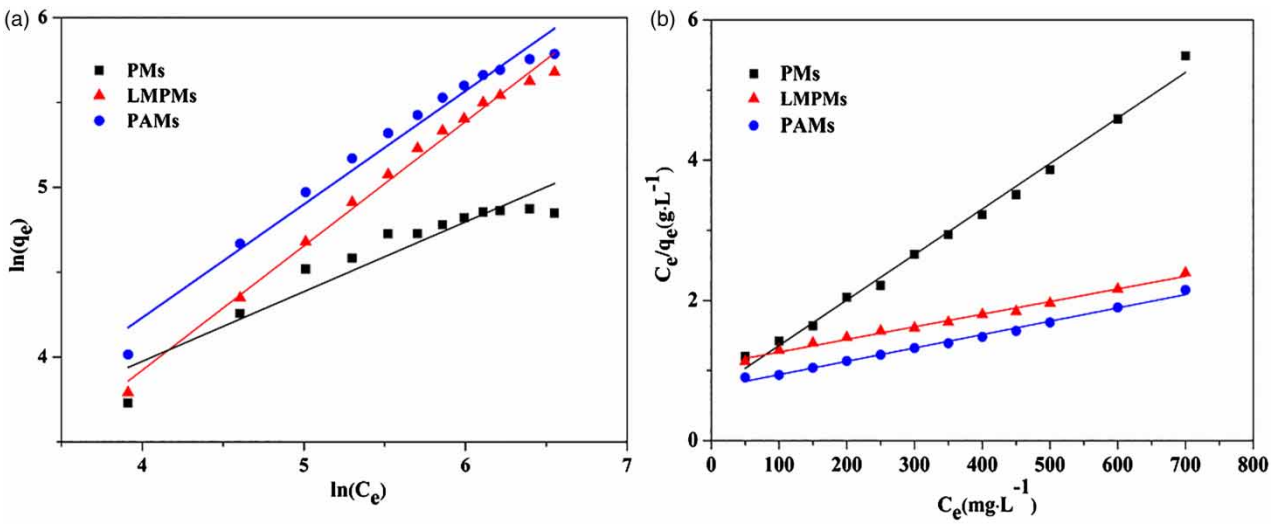

Figure 5 | The linear fit of the Langmuir isotherm (a) and Freundlich isotherm (b).

Bonding mode

A possible reaction mechanism diagram was proposed. According to the 'egg-box' model proposed for the metal-binding mechanism of pectin (Grant *et al.* 1973), a coordination bond is formed between M^{2+} (M^{2+} stands for Pb(II) or Cd(II)) and hydroxy and carboxyl and a chelate is formed. At slightly acid pH, –COOH and –OH groups on microspheres donated their electron pairs to M^{2+} to form complex through coordination covalent bond. In addition, the results from EDS exhibited that the content of Pb was increased and that of Ca(II) decreased apparently, indicating a ligand-exchange between the coordinated Ca(II) and Pb(II) (Mata *et al.* 2009). Thus, pectin with a low DE presumably exerts considerably higher metal-binding activity.

Selective adsorption

The result of the selective adsorption of PMs, LMPMs and PAMs for Cd(II) and Pb(II) was shown in Figure 4(d). It was obvious that the adsorption for Pb(II) was better than that for Cd(II) in the binary metal ion solution, which could be explained by the covalent index $X_m{}^2r$ (X_m stands for electronegativity, r stands for ionic radius) (Zhang *et al.* 2017a). Generally, the greater the $X_m{}^2r$ value is, the more the covalent bonds between the adsorbent and the metal ions form, and the larger the adsorption capacity on the adsorbent surface is (Nieboer & Richardson 1980). According to hard and soft acids and bases (HSAB) theory (Alfarra *et al.* 2004), the higher the $X_m{}^2r$ value was, the more the characteristics of soft acid was presented. Pb(II) ion belonged to soft ion that tended to combine with hydroxyl on microspheres, while Cd(II) belonged to intermediate ion that was of less binding capacity with amino groups than Pb(II).

Desorption and regeneration

The adsorption-desorption tests were repeated five times in a binary ion mixture system, and the results were shown in Figure 6. However, the adsorption capacities of LMPMs and PAMs for Pb(II) were 122.72 $mg{\cdot}g^{-1}$ and 143.47 $mg{\cdot}g^{-1}$ even at the 5th recycle with the existence of Cd(II). The gradual and slight decrease of removal efficiency with the increase of reusing time might be due to the gradual saturation of adsorption sites by the metal ions (Kyzas *et al.* 2014). These results above indicated that LMPMs and PAMs were of desirable reusability and stable chemical property under the experimental conditions.

CONCLUSIONS

In this work, PMs, LMPMs and PAMs were successfully fabricated through crosslinking with calcium ion. SEM indicated a uniformly morphology and microstructure among PMs, LMPMs and PAMs. In adsorption tests, compared with that of PMs (127 $mg{\cdot}g^{-1}$), the maximum adsorption capacity for Pb(II) of LMPMs (292 $mg{\cdot}g^{-1}$) increased to 2.29 times and of PAMs (325 $mg{\cdot}g^{-1}$) increased about 2.6 times which implied that the adsorption ability of PAMs was improved efficiently by decreasing the DE. The selective adsorption capacity for Pb(II) of PAMs was better than Cd(II) in the binary metal ion solution. The experimental data were well fitted with the

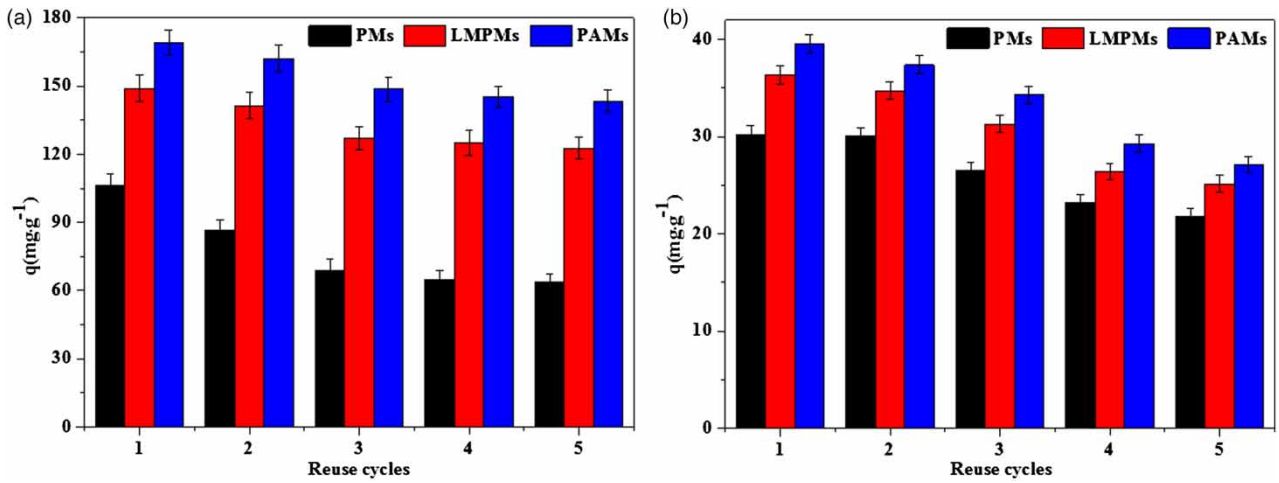

Figure 6 | Results of five times adsorption-desorption for the reuse of microspheres for Pb(II) (a) and Cd(II) (b) adsorption.

pseudo-second-order kinetic and the Langmuir isotherm models, indicating that the adsorption process was mainly a monolayer adsorption and chemisorption. In addition, the result of regeneration experiments indicated the removal efficiency for Pb(II) of PAMs was more than 54% after five adsorption-desorption cycles in a binary ion mixture system. Nowadays, researchers have modified pectin by grafting, saponification and cross-linking to improve their adsorption capacity. Liang *et al.* (Sha *et al.* 2010) saponified and hydrolyzed pectin and ion-crosslinked with K^+, then its adsorption quantity on copper ions was 59.77 $mg{\cdot}g^{-1}$. Liang *et al.* (Feng & Guo 2012) saponified pectin and ion-crosslinked with Ca^{2+}; after adsorption the removal rate of Cu^{2+}, Pb^{2+} and Zn^{2+} was 70.7 $mg{\cdot}g^{-1}$, 209.8 $mg{\cdot}g^{-1}$ and 56.2 $mg{\cdot}g^{-1}$, respectively. Schiewer and Balaria (Schiewer & Balaria 2009) processed and grinded orange peels to adsorb the lead ions in aqueous solutions with a removal rate of up to 90%. In this study, the method of modifying pectin is simple and fast and PAMs was efficient in removing Pb(II) from aqueous solution with a high adsorption rate of up to 96% (325 $mg{\cdot}g^{-1}$). Moreover, high selective for Pb(II) of PAMs was showed in mixed aqueous solution of Cd(II) and Pb(II). Besides, microspheres are convenient for separation and facilitate reusing operation. All the results above implied that the newly prepared PAMs might be the promising adsorbent for wastewater treatment.

ACKNOWLEDGEMENTS

This work was supported by Scientific Research Foundation for Returned Scholars (Ministry of Education of China,201503), Opening Foundation of Key Laboratory of Resource Biology and Biotechnology in Western China (Northwest University, Ministry of Education), Natural Science Basic Research Plan in Shaanxi Province of China (2017JM2016) and National Natural Science Foundation of China (81673115).

REFERENCES

Afanas'Ev, S. P., Panova, É. P., Katseva, G. N., Kukhta, E. P. & Chirva, V. Y. 1984 Modification of the titrimetric method of analyzing pectin substances. *Chemistry of Natural Compounds* **20** (4), 404–406.

Alfarra, A., Frackowiak, E. & Béguin, F. 2004 The HSAB concept as a means to interpret the adsorption of metal ions onto activated carbons. *Applied Surface Science* **228** (1), 84–92.

Assifaoui, A., Lerbret, A., Uyen, H. T. D., Neiers, F., Chambin, O., Loupiac, C. & Cousin, F. 2015 Structural behaviour differences in low methoxy pectin solutions in the presence of divalent cations (Ca^{2+} and Zn^{2+}): a process driven by the binding mechanism of the cation with the galacturonate unit. *Soft Matter* **11** (3), 551–560.

Blumenthal, N. C., Cosma, V., Skyler, D., Legeros, J. & Walters, M. 1995 The effect of cadmium on the formation and properties of hydroxyapatite in vitro and its relation to cadmium toxicity in the skeletal system. *Calcified Tissue International* **56** (4), 316–322.

Celus, M., Kyomugasho, C., Kermani, Z. J., Roggen, K., Loey, A. M. V., Grauwet, T. & Hendrickx, M. E. 2017 Fe^{2+} adsorption on citrus pectin is influenced by the degree and pattern of methylesterification. *Food Hydrocolloids* **73**, 101–109.

Chen, C. & Wang, J. 2008 Removal of Pb^{2+}, Ag^{+}, Cs^{+} and Sr^{2+} from aqueous solution by brewery's waste biomass. *Journal of Hazardous Materials* **151** (1), 65–70.

Chojnacka, K. 2010 Biosorption and bioaccumulation–the prospects for practical applications. *Environment International* **36** (3), 299–307.

Dineshkumar, M., Jasaswini, T., Abhishek, S., Madanmohan, M. & Kunj, B. 2008 Graft copolymer (chitosan-g-N-vinyl formamide): synthesis and study of its properties like swelling, metal ion uptake and flocculation. *Carbohydrate Polymers* **74** (3), 632–639.

Dragan, E. S., Apopei Loghin, D. F. & Cocarta, A. I. 2014a Efficient sorption of Cu^{2+} by composite chelating sorbents based on potato starch-graft-polyamidoxime embedded in chitosan beads. *ACS Applied Materials & Interfaces* **6** (19), 16577–16592.

Dragan, E. S., Cocarta, A. I. & Dinu, M. V. 2014b Facile fabrication of chitosan/poly(vinyl amine) composite beads with enhanced sorption of Cu^{2+}. Equilibrium, kinetics, and thermodynamics. *Chemical Engineering Journal* **255** (6), 659–669.

España, J. S., Pamo, E. L., Pastor, E. S., Andrés, J. R. & Rubí, J. A. M. 2006 The removal of dissolved metals by hydroxysulphate precipitates during oxidation and neutralization of acid mine waters, iberian pyrite belt. *Aquatic Geochemistry* **12** (3), 269–298.

Feng, N C. & Guo, X Y. 2012 Characterization of adsorptive capacity and mechanisms on adsorption of copper, lead and zinc by modified orange peel. *Transactions of the Nonferrous Metals Society of China* **22** (5), 1224–1231.

Fonseca, M. G. D., Oliveira, M. M. D., Arakaki, L. N. H., Espinola, J. G. P. & Airoldi, C. 2005 Natural vermiculite as an exchanger support for heavy cations in aqueous solution. *Journal of Colloid & Interface Science* **285** (1), 50–55.

Grant, G. T., Morris, E. R., Rees, D. A., Smith, P. J. C. & Thom, D. 1973 Biological interactions between polysaccharides and divalent cations: the egg-box model. *FEBS Letters* **32** (1), 195–198.

Ilse, F., Eugénie, D., Thomas, D., Paula, M., Ann, V. L. & Marc, H. 2009 Influence of intrinsic and extrinsic factors on rheology of pectin-calcium gels. *Food Hydrocolloids* **23** (8), 2069–2077.

Iqbal, M., Saeed, A. & Zafar, S. I. 2009 FTIR spectrophotometry, kinetics and adsorption isotherms modeling, ion exchange, and EDX analysis for understanding the mechanism of Cd^{2+} and Pb^{2+} removal by mango peel waste. *Journal of Hazardous Materials* **164** (1), 161–171.

Jorgetto, A. D. O., Silva, A. C. P. D., Wondracek, M. H. P., Silva, R. I. V., Velini, E. D., Saeki, M. J., Pedrosa, V. A. & Castro, G. R. 2015 Multilayer adsorption of Cu(II) and Cd(II) over Brazilian Orchid Tree (Pata-de-vaca) and its adsorptive properties. *Applied Surface Science* **345**, 81–89.

Khormaei, M., Nasernejad, B., Edrisi, M. & Eslamzadeh, T. 2007 Copper biosorption from aqueous solutions by sour orange residue. *Journal of Hazardous Materials* **149** (2), 269–274.

Khotimchenko, M. Y., Kolenchenko, E. A. & Khotimchenko, Y. S. 2008 Zinc-binding activity of different pectin compounds in aqueous solutions. *Journal of Colloid & Interface Science* **323** (2), 216–222.

Kyzas, G. Z., Siafaka, P. I., Lambropoulou, D. A., Lazaridis, N. K. & Bikiaris, D. N. 2014 Poly(itaconic acid)-grafted chitosan adsorbents with different cross-linking for Pb(II) and Cd(II) uptake. *Langmuir the ACS Journal of Surfaces & Colloids* **30** (1), 120–131.

Li, M. & Buschle-Diller, G. 2017 Pectin-blended anionic polysaccharide films for cationic contaminant sorption from water. *International Journal of Biological Macromolecules* **101**, 481–489.

Liao, B., Sun, W. Y., Guo, N., Ding, S. L. & Su, S. J. 2016 Comparison of Co^{2+} adsorption by chitosan and its triethylene-tetramine derivative: performance and mechanism. *Carbohydrate Polymers* **151**, 20–28.

Liu, L., Fishman, M. L., Kost, J. & Hicks, K. B. 2003 Pectin-based systems for colon-specific drug delivery via oral route. *Biomaterials* **24** (19), 3333–3343.

Mata, Y. N., Blázquez, M. L., Ballester, A., González, F. & Muñoz, J. A. 2009 Sugar-beet pulp pectin gels as biosorbent for heavy metals: preparation and determination of biosorption and desorption characteristics. *Chemical Engineering Journal* **150** (2–3), 289–301.

Mohammadi, T., Moheb, A., Sadrzadeh, M. & Razmi, A. 2005 Modeling of metal ion removal from wastewater by electrodialysis. *Separation & Purification Technology* **41** (1), 73–82.

Mortaheb, H. R., Zolfaghari, A., Mokhtarani, B., Amini, M. H. & Mandanipour, V. 2010 Study on removal of cadmium by hybrid liquid membrane process. *Journal of Hazardous Materials* **177** (1–3), 660–667.

Nieboer, E. & Richardson, D. H. S. 1980 The replacement of the nondescript term 'heavy metals' by a biologically and chemically significant classification of metal ions. *Environmental Pollution* **1** (1), 3–26.

Panda, G. C., Das, S. K. & Guha, A. K. 2008 Biosorption of cadmium and nickel by functionalized husk of Lathyrus sativus. *Colloids & Surfaces B Biointerfaces* **62** (2), 173–179.

Rice, K. M., Walker Jr., E. M., Wu, M., Gillette, C. & Blough, E. R. 2014 Environmental mercury and its toxic effects. *Journal of Preventive Medicine & Public Health* **47** (2), 74–83.

Schiewer, S. & Balaria, A. 2009 Biosorption of Pb^{2+} by original and protonated citrus peels: equilibrium, kinetics, and mechanism. *Chemical Engineering Journal* **146** (2), 211–219.

Serguschenko, I., Kolenchenko, E. & Khotimchenko, M. 2007 Low esterified pectin accelerates removal of lead ions in rats. *Nutrition Research* **27** (10), 633–639.

Sha, L., Guo, X., Feng, N. & Tian, Q. 2010 Isotherms, kinetics and thermodynamic studies of adsorption of Cu^{2+} from aqueous solutions by Mg^{2+}/K^{+} type orange peel adsorbents. *Journal of Hazardous Materials* **174** (1), 756–762.

Shariful, M. I., Sharif, S. B., Lee, J. J. L., Habiba, U., Ang, B. C. & Amalina, M. A. 2017 Adsorption of divalent heavy metal ion by mesoporous-high surface area chitosan/poly (ethylene oxide) nanofibrous membrane. *Carbohydrate Polymers* **157**, 57–64.

Wang, J. & Chen, C. 2014 Chitosan-based biosorbents: modification and application for biosorption of heavy metals and radionuclides. *Bioresource Technology* **160** (5), 129–141.

Yang, G., Tang, L., Lei, X., Zeng, G., Cai, Y., Wei, X., Zhou, Y., Li, S., Fang, Y. & Zhang, Y. 2014 Cd(II) removal from aqueous solution by adsorption on α-ketoglutaric acid-modified magnetic chitosan. *Applied Surface Science* **292**, 710–716.

Zhang, H., Dang, Q., Liu, C., Cha, D., Yu, Z., Zhu, W. & Bing, F. 2017a Uptake of Pb(II) and Cd(II) on chitosan microsphere surface successively grafted by methyl acrylate and diethylenetriamine. *ACS Applied Materials & Interfaces* **9** (12), 11144–11155.

Zhang, Q., Li, Y., Yang, Q., Chen, H., Chen, X., Jiao, T. & Peng, Q. 2017b Distinguished Cr(VI) capture with rapid and superior capability using polydopamine microsphere: behavior and mechanism. *Journal of Hazardous Materials* **342**, 732–740.

First received 27 June 2018; accepted in revised form 14 April 2019. Available online 30 April 2019